Rapid Communications

Origin of skyrmion lattice phase splitting in Zn-substituted Cu_2OSeO_3

A. Štefančič,[1,*] S. H. Moody,[2] T. J. Hicken,[2] M. T. Birch,[2] G. Balakrishnan,[1] S. A. Barnett,[3] M. Crisanti,[1,4] J. S. O. Evans,[5] S. J. R. Holt,[1] K. J. A. Franke,[2] P. D. Hatton,[2] B. M. Huddart,[2] M. R. Lees,[1] F. L. Pratt,[6] C. C. Tang,[3] M. N. Wilson,[2] F. Xiao,[7,8] and T. Lancaster[2,†]

[1]*University of Warwick, Department of Physics, Coventry CV4 7AL, United Kingdom*
[2]*Durham University, Department of Physics, South Road, Durham DH1 3LE, United Kingdom*
[3]*Diamond Light Source, Harwell Science and Innovation Campus, Didcot OX11 0DE, United Kingdom*
[4]*Institut Laue-Langevin, Large Scale Structures Group, 71 Avenue des Martyrs CS 20156, 38042 Grenoble, Cedex 9, France*
[5]*Durham University, Department of Chemistry, South Road, Durham DH1 3LE, United Kingdom*
[6]*ISIS Facility, STFC Rutherford Appleton Laboratory, Chilton Didcot, Oxfordshire OX11 0QX, United Kingdom*
[7]*Laboratory for Neutron Scattering, Paul Scherrer Institut, CH-5232 Villigen PSI, Switzerland*
[8]*Department of Chemistry and Biochemistry, University of Bern, CH-3012 Bern, Switzerland*

(Received 12 July 2018; published 8 November 2018)

We present an investigation into the structural and magnetic properties of Zn-substituted Cu_2OSeO_3, a system in which the skyrmion lattice (SkL) phase in the magnetic field–temperature phase diagram was previously seen to split as a function of increasing Zn concentration. We find that splitting of the SkL is only observed in polycrystalline samples and reflects the occurrence of several coexisting phases with different Zn content, each distinguished by different magnetic behavior. No such multiphase behavior is observed in single-crystal samples.

DOI: 10.1103/PhysRevMaterials.2.111402

There has been considerable recent interest in the synthesis and understanding of materials hosting topological phases, owing to their exotic physics and potential for applications. Skyrmions are nano-sized, topologically protected magnetic spin textures, which are promising candidates for energy-efficient, high-density storage devices [1–3]. Skyrmions are found in a number of systems including MnSi [4,5], $Fe_{1-x}Co_xSi$ [6–8], FeGe [9], β-Mn–type Co-Zn-Mn alloys [10], Cu_2OSeO_3 [11], GaV_4S_8 [12], and GaV_4Se_8 [13]. The discovery of skyrmions in the multiferroic insulator Cu_2OSeO_3 represents an important milestone, because of the possibility of manipulating them with an external electric field [11,14–16]. Despite an intensive search, the number of known skyrmion-hosting materials still remains relatively small, owing to the very specific structural properties (absence of inversion center) and magnetic properties (ferromagnetism and presence of Dzyaloshinskii-Moriya interactions) needed to promote the formation of magnetic skyrmions. An alternative route to expand the number of skyrmionic materials is to utilize a chemical doping/substitution strategy in known skyrmion-hosting systems. This approach has recently been adopted in Cu_2OSeO_3, where Zn substitution led to observation of splitting of the skyrmion lattice (SkL) phase into two distinct pockets [17], and Ni substitution led to an expansion of the SkL phase [18].

Cu_2OSeO_3 crystallizes in the noncentrosymmetric cubic $P2_13$ space group [19]. Two crystallographically inequivalent Cu^{2+} cations in trigonal bipyramidal and square pyramidal coordination geometry (designated as $Cu^{\rm I}$ and $Cu^{\rm II}$, respectively) are present in a ratio 1:3. These have spins $S = 1/2$ pointing in opposite directions forming a ferrimagnetic lattice [20–22]. Magnetic interactions between spins are mediated through oxygen atoms via ferromagnetic and antiferromagnetic superexchange interactions [23,24]. As reported by Wu *et al.* [17], the magnetic moment of Cu_2OSeO_3 monotonically decreases with increasing Zn-substitution levels, which they interpret in terms of the site-specific substitution of Cu^{2+} cation at the $Cu^{\rm II}$ site with nonmagnetic Zn^{2+}. This is accompanied by a splitting of the SkL phase observed in pristine Cu_2OSeO_3 into two distinct pockets.

In order to understand the effect of substitution and to confirm the origin of the SkL splitting in this system, investigations on high-quality single crystals are essential. We have produced single crystals of Zn-substituted Cu_2OSeO_3 for several substitution levels of Zn, allowing us to compare their behavior to that of high-purity polycrystalline materials. We find that the splitting of the SkL phase reflects the presence of multiple structural phases in polycrystalline samples. In contrast, phase-pure single-crystal samples do not show such behavior.

By utilizing the chemical vapor phase transport technique, single crystals of Zn-substituted Cu_2OSeO_3, with nominal 2%, 8%, and 12% Zn content, were grown. Energy-dispersive x-ray spectroscopy (EDX), x-ray fluorescence (XRF), and inductively coupled plasma mass spectroscopy (ICP MS) measurements on single crystals revealed the Zn concentrations given in Table I. We use the average values of Zn substitution (0.5%, 1.8%, and 2.4%) below.

Structural analysis of the single-crystal samples was carried out using the high resolution I19 beamline at the Diamond Light Source as described in the Supplemental Material [25–32]. The a lattice parameter, extracted from data collected at the Zr K edge (17.9976 keV), was found to monotonically

*A.Stefancic@warwick.ac.uk
†tom.lancaster@durham.ac.uk

TABLE I. Percentage of Zn concentration in $(Cu_{1-x}Zn_x)_2OSeO_3$ single crystals determined by ICP MS, EDX, and XRF. Zn concentration in corresponding polycrystalline samples is given in the rightmost column.

Nominal	ICP MS	EDX	XRF	Average	Polycrystal
2	0.9	0.52(9)	0.12(1)	0.5	2.0
8	1.9	1.71(4)	1.71(1)	1.8	6.4
12	2.4	2.51(3)	2.26(1)	2.4	10.5

increase with increasing Zn substitution levels, as expected when substituting Cu^{2+} with the slightly larger Zn^{2+} cations (with atomic radii of 0.65 and 0.68 Å for five coordinate Cu^{2+}/Zn^{2+}, respectively [33]). A close comparison of the structural models for pristine Cu_2OSeO_3 single crystals and 2.4% Zn-substituted Cu_2OSeO_3 revealed a very subtle increase of the short Cu^{I}-O1 and Cu^{II}-O2 bond distances of 0.004(2) and 0.002(2) Å, respectively (Fig. 1). This leads to an increase of Cu^{I}-Cu^{II} distances, while the Cu^{II}-Cu^{II} distances remain the same [25].

Polycrystalline materials were synthesized as reported in the Supplemental Material [25]. The phase-purity and lattice parameters were investigated using high-resolution powder x-ray diffraction (PXRD) at the I11 beamline, Diamond Light Source [25,34], with diffraction patterns for each Zn-substituted polycrystalline samples measured at 15.02 keV. A simple axial model was used to describe the peak asymmetry at low angles arising from axial divergence of the beam and a pseudo-Voigt function to describe the Cu_2OSeO_3 peak shapes.

In the unsubstituted material, a single phase of Cu_2OSeO_3 is sufficient to model the diffraction pattern, with small residuals. However, for the samples with increased substitution levels, all of the peaks in the diffraction pattern split, as shown in Figs. 2(b) to 2(f). Refinements revealed that this splitting could only be effectively modeled by the inclusion of two or three distinct Cu_2OSeO_3 phases with differing lattice parameters, suggesting that the polycrystalline materials are multiphase under the synthesis conditions used.

Based on our refinements, the lattice parameter a and cell volume of each phase increases monotonically with increasing Zn-substitution levels (Fig. 4), consistent with the behavior of the single crystals. Using our PXRD measurements, the

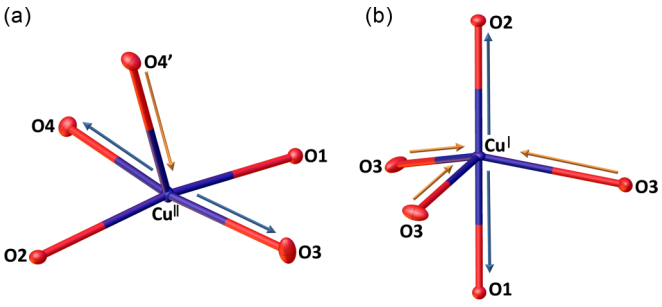

FIG. 1. Structural model for 2.4% Zn-substituted Cu_2OSeO_3. Coordination environment of (a) the Cu^{II} site (square pyramidal) and (b) the Cu^{I} site (trigonal bipyramidal). Arrows indicate elongation and contraction of bond distances compared to pristine Cu_2OSeO_3.

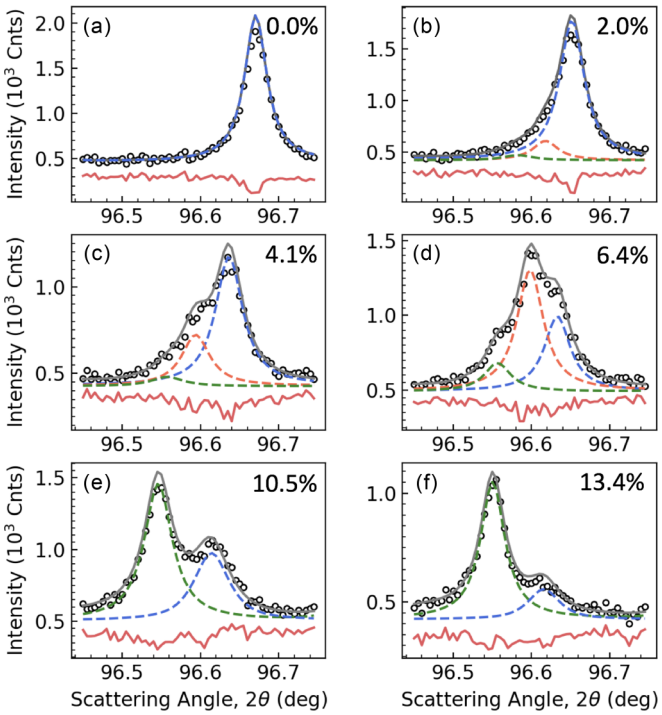

FIG. 2. Powder x-ray diffraction peak at $2\theta = 96.65^\circ$ for polycrystalline samples with different Zn concentrations. Open circles: experimental data; dashed lines: single peak fits for individual phases; gray solid line: a sum of these fits; red line: difference between the global fit and the data. This demonstrates that the asymmetrical shape and splitting of diffraction peaks can only be modeled by multiple phases.

estimated Zn-substitution levels in polycrystalline samples are taken as 0%, 2%, 4.1%, 6.4%, 7.9%, 10.5%, and 13.4%, for the nominal starting compositions of 0%, 2%, 5%, 8%, 10%, 12%, and 15%, respectively [25]. The substitution level of Cu^{2+} with Zn^{2+} is higher at low nominal substitution values (up to 5% Zn), while above this level it starts to decrease. This decrease is reflected in the amount of unreacted CuO detected with powder diffraction, increasing from 1% in the sample with 6.4% Zn up to 5% in the sample with 13.4% Zn-substitution level. The crystal structure of Zn_2OSeO_3, if it exists, is not known, therefore the increase of unreacted CuO with increasing Zn-substitution levels can be related to the stability and Zn^{2+} uptake ability of the Cu_2OSeO_3 crystal structure. In addition, up to 3% of a Zn_2SiO_4 impurity phase was observed in samples with Zn-substitution levels higher than 4%, indicating that ZnO reacts with silica tubes (although we would normally expect this reaction to occur at higher temperatures of $>1000\,^\circ$C [35]). The estimated Zn concentrations are given in Table I for comparison with the single-crystal samples. We note that the Zn uptake is far smaller in the single-crystal samples, compared to the polycrystalline analogs.

To characterize the magnetic behavior of all samples, dc magnetic susceptibility measurements were carried out using zero-field-cooled and field-cooled protocols. Single crystals were aligned with the applied magnetic field directed along the [111] direction. The resulting magnetization curves are

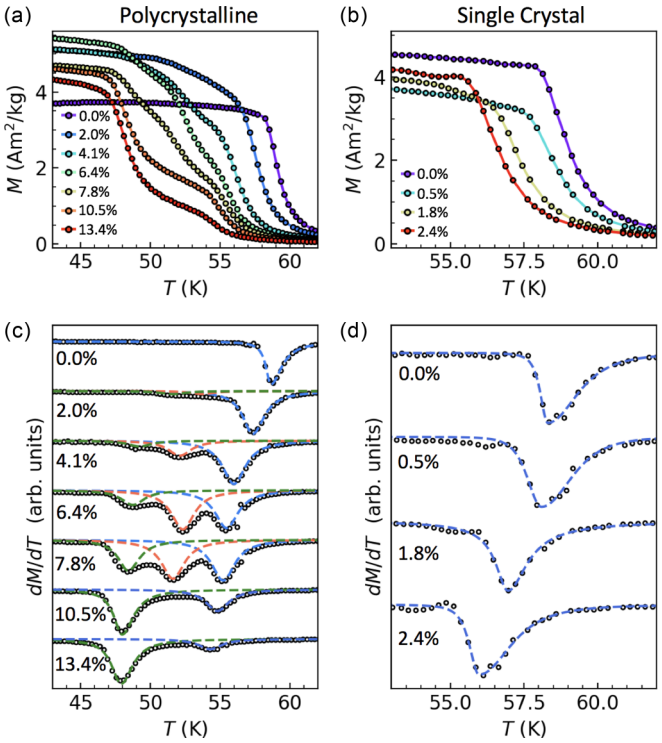

FIG. 3. (a) Magnetization M vs T for polycrystalline samples, measured in a magnetic field of 25 mT. (b) The same for single-crystal samples. (c) The temperature derivative of M vs T for polycrystalline samples, revealing multiple magnetic transitions. (Open circles: experientially obtained data; blue, orange, and green dotted lines: fits to distinct magnetic phases.) (d) The temperature derivative of the M vs T single-crystal data, showing a single transition.

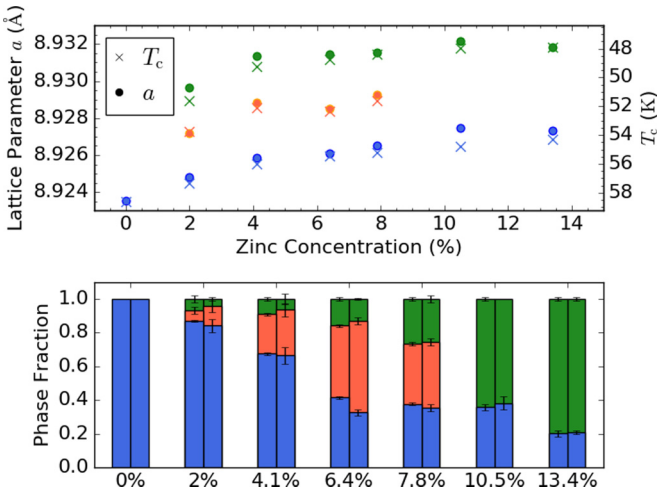

FIG. 4. Top: Critical temperature T_c (crosses) and lattice parameter a (circles) for each Cu_2OSeO_3 phase in polycrystalline samples, as a function of Zn substitution. Bottom: Volume fractions of each distinct phase in polycrystalline samples extracted from x-ray and dc magnetometry data.

shown in Figs. 3(a) and 3(b). In single crystals the magnetic transition temperature T_c is found to decrease with increasing Zn content. The decrease in T_c seen in single crystals is comparable to that observed in polycrystalline materials for the same actual Zn-substitution levels. The steplike nature of the data for the polycrystalline material suggests that there are multiple magnetic transitions occurring. This is more clearly seen in the derivative of these data [Fig. 3(c)], which show multiple peaks, particularly for higher Zn substitution, indicating the presence of several magnetic phases with different values of T_c. (This may be contrasted with analogous measurements on single crystals [Fig. 3(d)] showing a single transition.) By fitting the peaks a critical temperature T_c and volume fraction for each distinct phase was determined, as summarized in Fig. 4.

The existence of skyrmions, along with the size and potential splitting of the skyrmion pocket, were investigated using ac magnetic susceptibility. The resulting magnetic phase diagrams are presented in Fig. 5, where we show the real component χ' as a function of applied field and temperature, which provides a good indication of the helical, conical, and skyrmion structures. The phase diagrams for polycrystalline samples closely resemble the data from Wu *et al.*, with T_c of the sample decreasing with increasing Zn substitution, while the skyrmion region seemingly splits into two (or even three in, for example, the case of the 6.4% substituted sample) distinct pockets. (This is also seen in the imaginary component of the susceptibility χ'' [25].) Data measured on single crystals [Figs. 5(e)–5(h)], show a single skyrmion phase in each of the samples. The skyrmion pockets in single crystals with 0.5%, 1.8%, and 2.4% Zn-substitution levels stretch from 54.75 to 57.25 K, 53.5 to 56 K, and 52.75 to 55 K, respectively. Although the pockets shift to lower temperatures with increasing Zn concentration, their widths remain roughly constant (between 2.25 and 2.5 K), in contrast to the skyrmion pockets detected in polycrystalline materials. Single crystals with 2.4% Zn-substitution level were also measured with B || to [110] and the only noticeable differences are in the shape and size of the skyrmion pocket as reported in the literature [36]. For B || to [111], the skyrmion pocket can be found in the temperature range between 52.75 and 55.0 K, while for B || to [110] the pocket exists from 53.25 to 55.0 K.

Our analysis of the magnetization measurements suggests the presence of multiple magnetic phases in the polycrystalline samples. To establish whether these are intrinsic to each material, we carried out longitudinal field (LF) muon-spin relaxation (μSR) measurements on polycrystalline samples, since the muon is a sensitive local probe of magnetism [37]. In order to parametrize the spectra across the measured temperature regime, they were fitted to an exponential function, with the resulting values of relaxation rate λ shown in Fig. 6. We find λ to be significantly larger inside the SkL phase than outside it. Notably, we observe peaks in λ coinciding with the SkL phases which are significantly broader than the typical peaks that indicate transitions between long-range ordered and paramagnetic phases (shown in Ref. [25]). This suggests that emergent dynamics in the SkL phase enhance λ. In both 6.4% and 10.5% Zn-substituted materials we see two peaks which coincide with the SkL regions identified above. To estimate the correlation time for dynamics in the local magnetic field distribution in the SkL phases, we compared these results and further transverse field μSR measurements on 6.4% Zn-substituted Cu_2OSeO_3. From these [25,38] we estimate that the correlation time in the SkL phase is of order $\tau \approx 100$ ns, compared to ≈ 30 ns in the conical phase. This

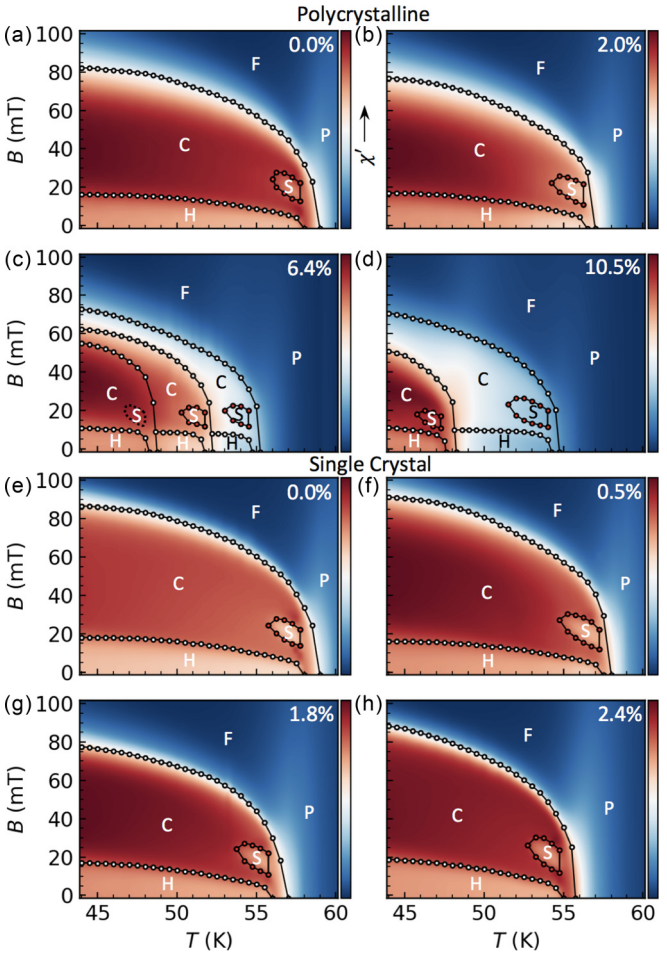

FIG. 5. (a)–(d) Real component of ac susceptibility χ' at a frequency of 10 Hz and driving field of 0.3 mT as a function of field B and temperature T for polycrystalline samples, showing the paramagnetic (P), ferrimagnetic (F), conical (C), helical (H), and skyrmion lattice (S) phases. (e)–(h) The same, but for single-crystal samples.

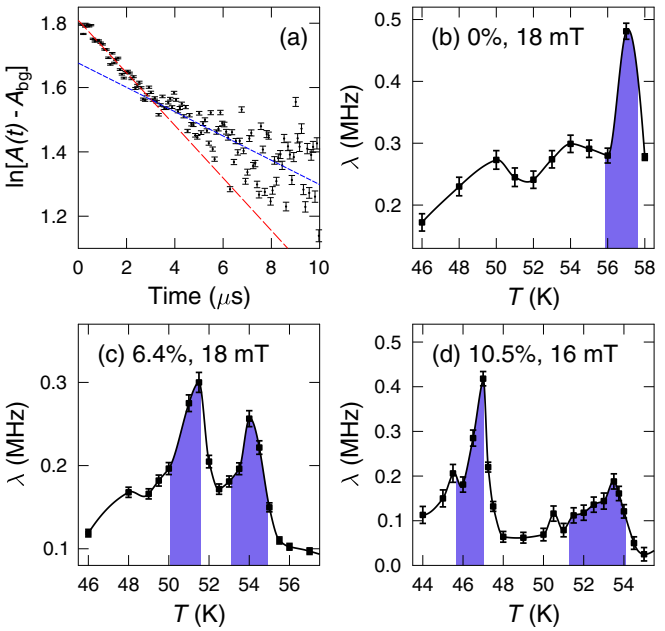

FIG. 6. (a) LF μSR spectra for 6.4% Zn-substituted polycrystalline Cu_2OSeO_3 measured at 54 K in 18 mT on a logarithmic scale with the background subtracted. Lines are guides to the eye. Relaxation rate λ for LF μSR measurements of (b) pristine, (c) 6.4%, and (d) 10.5% Zn-substituted Cu_2OSeO_3. Shaded regions indicate the location of the SkL phase derived from ac susceptibility.

possibly reflects an increase in spin stiffness in the SkL phase compared to the surrounding magnetic phases.

Closer examination of the spectra measured for 6.4% Zn substitution near the peaks in λ suggests that they are better described by the sum of two exponential functions with distinct relaxation rates λ_i. This is seen in Fig. 6(a), where data plotted on a logarithmic scale shows two approximately linear regimes (separated by a crossover at $\approx$2.5 μs) with significantly different gradients, suggesting that a two-exponential model provides a more accurate description of the data. This strongly implies the occurrence of two magnetically and spatially distinct classes of muon site, with different correlation times, since if there were only one muon site subject to fluctuations with two correlation times, the slower one would dominate, leading to a single relaxation rate [39]. Moreover, we expect both classes of muon site to occur in the bulk of the material. For comparison, the same analysis was also carried out on LF μSR data measured on a polycrystalline sample of pristine Cu_2OSeO_3 (where only one peak is seen). Here, a single exponential function models the data best, suggesting that there is only one magnetically distinct muon site in this material. These measurements therefore provide unambiguous evidence for the coexistence of at least two magnetic phases in the bulk of polycrystalline Zn-substituted Cu_2OSeO_3.

Evidence for multiple phases in polycrystalline samples has come from structural and magnetic measurements. We may link these with the observation of a correlation between the lattice parameter and T_c for each phase in the polycrystalline samples. These are plotted in Fig. 4(a), labeled by Zn substitution. The fractional volume of each phase was also determined by both Rietveld refinement and magnetometry and is shown in Fig. 4(b). There is good agreement between the two datasets. We therefore conclude that the polycrystalline Zn-substituted Cu_2OSeO_3 samples are multiphase, featuring multiple, distinct Zn-substituted Cu_2OSeO_3 phases. This then explains the origin of the split skyrmion pocket: each distinct phase exhibits the skyrmion spin structure at a different temperature, reflecting the differing values of T_c.

The synthesis conditions for our polycrstalline samples are similar to those employed by Wu *et al.* However, when we subsequently prolonged the reaction times to 4 weeks, we found that, while additional phases are formed, one majority phase starts to become dominant. We believe that employing sufficiently long reaction periods should cause all the additional phases to eventually converge into one thermodynamically stable phase (see Ref. [25]).

Although the estimated Zn content in our single-crystal samples is, at most, 2.4% and so we might not expect to resolve any splitting in the skyrmion phase, we note that in the 2.0% substituted polycrystalline sample there is evidence for both structural and magnetic phase separation. We see

no evidence for multiphase behavior in our single crystals, suggesting that these are composed of a single phase with a single magnetic transition and should be expected to host a single skyrmion lattice phase.

In conclusion, we have shown that the splitting of the SkL phase observed exclusively in polycrystalline samples reflects the system's splitting into multiple Zn-substituted phases, each characterized by different magnetic behavior. The occurrence of these multiple phases can probably be eliminated by employing suitably extended reaction times during synthesis. Our results demonstrate the importance of high-quality single-crystal samples in the investigation of the magnetic properties of skyrmion-hosting systems.

Data will be made available via Warwick Research Archive Portal [40].

This work is financially supported by EPSRC (EP/N032128/1). Part of this work was performed at the Science and Technology Facilities Council (STFC) ISIS Facility, Diamond Light Source and the Swiss Muon Source, Paul Scherrer Institut. We are grateful for the provision of beamtime. We thank Matthias Gutmann (ISIS, UKRI, STFC) for useful discussions, Geoff West, Samuel Marks and Reza Kashtiban (University of Warwick) for help with EDX analysis and Joel Barker (Swiss Muon Source) for assistance with muon measurements.

[1] J. P. Liu, Z. Zhang, and G. Zhao, *Skyrmions: Topological Structures, Properties, and Applications* (CRC Press, Boca Raton, FL, 2016).
[2] N. Nagaosa and Y. Tokura, Nat. Nanotechnol. **8**, 899 (2013).
[3] A. Fert, V. Cros, and J. Sampaio, Nat. Nanotechnol. **8**, 152 (2013).
[4] S. Mühlbauer, B. Binz, F. Jonietz, C. Pfleiderer, A. Rosch, A. Neubauer, R. Georgii, and P. Böni, Science **323**, 915 (2009).
[5] A. Tonomura, X. Yu, K. Yanagisawa, T. Matsuda, Y. Onose, N. Kanazawa, H. S. Park, and Y. Tokura, Nano Lett. **12**, 1673 (2012).
[6] W. Münzer, A. Neubauer, T. Adams, S. Mühlbauer, C. Franz, F. Jonietz, R. Georgii, P. Böni, B. Pedersen, M. Schmidt, A. Rosch, and C. Pfleiderer, Phys. Rev. B **81**, 041203 (2010).
[7] X. Yu, Y. Onose, N. Kanazawa, J. Park, J. Han, Y. Matsui, N. Nagaosa, and Y. Tokura, Nature (London) **465**, 901 (2010).
[8] L. J. Bannenberg, K. Kakurai, F. Qian, E. Lelièvre-Berna, C. D. Dewhurst, Y. Onose, Y. Endoh, Y. Tokura, and C. Pappas, Phys. Rev. B **94**, 104406 (2016).
[9] X. Yu, N. Kanazawa, Y. Onose, K. Kimoto, W. Zhang, S. Ishiwata, Y. Matsui, and Y. Tokura, Nat. Mater. **10**, 106 (2011).
[10] Y. Tokunaga, X. Yu, J. White, H. M. Rønnow, D. Morikawa, Y. Taguchi, and Y. Tokura, Nat. Commun. **6**, 7638 (2015).
[11] S. Seki, X. Yu, S. Ishiwata, and Y. Tokura, Science **336**, 198 (2012).
[12] I. Kézsmárki, S. Bordács, P. Milde, E. Neuber, L. Eng, J. White, H. M. Rønnow, C. Dewhurst, M. Mochizuki, K. Yanai *et al.*, Nat. Mater. **14**, 1116 (2015).
[13] Y. Fujima, N. Abe, Y. Tokunaga, and T. Arima, Phys. Rev. B **95**, 180410 (2017).
[14] J. S. White, I. Levatić, A. A. Omrani, N. Egetenmeyer, K. Prša1, I. Živković, J. L. Gavilano, J. Kohlbrecher, M. Bartkowiak, and H. Berger, J. Phys.: Condens. Matter **24**, 432201 (2012).
[15] J. S. White, K. Prša, P. Huang, A. A. Omrani, I. Živković, M. Bartkowiak, H. Berger, A. Magrez, J. L. Gavilano, G. Nagy, J. Zang, and H. M. Rønnow, Phys. Rev. Lett. **113**, 107203 (2014).
[16] J. S. White, I. Živković, A. J. Kruchkov, M. Bartkowiak, A. Magrez, and H. M. Rønnow, Phys. Rev. Appl. **10**, 014021 (2018).
[17] H. Wu, T. Wei, K. Chandrasekhar, T. Chen, H. Berger, and H. Yang, Sci. Rep. **5**, 13579 (2015).
[18] K. D. Chandrasekhar, H. Wu, C. Huang, and H. Yang, J. Mater. Chem. C **4**, 5270 (2016).
[19] H. Effenberger and F. Pertlik, Monatsh. Chem./Chem. Mon. **117**, 887 (1986).
[20] Jan-Willem G. Bos, C. V. Colin, and T. T. M. Palstra, Phys. Rev. B **78**, 094416 (2008).
[21] M. Belesi, I. Rousochatzakis, H. C. Wu, H. Berger, I. V. Shvets, F. Mila, and J.-P. Ansermet, Phys. Rev. B **82**, 094422 (2010).
[22] A. Maisuradze, Z. Guguchia, B. Graneli, H. M. Rønnow, H. Berger, and H. Keller, Phys. Rev. B **84**, 064433 (2011).
[23] J.-H. Yang, Z.-L. Li, X. Z. Lu, M.-H. Whangbo, S.-H. Wei, X. G. Gong, and H. J. Xiang, Phys. Rev. Lett. **109**, 107203 (2012).
[24] I. Živković, D. Pajić, T. Ivek, and H. Berger, Phys. Rev. B **85**, 224402 (2012).
[25] See Supplemental Material at http://link.aps.org/supplemental/10.1103/PhysRevMaterials.2.111402 for details of experimental methods, structural parameters, and further results of characterization from magnetometry and analysis of the μSR data.
[26] D. R. Allan, H. Nowell, S. A. Barnett, M. R. Warren, A. Wilcox, J. Christensen, L. K. Saunders, A. Peach, M. T. Hooper, L. Zaja *et al.*, Crystals **7**, 336 (2017).
[27] G. Winter, J. Appl. Crystallogr. **43**186 (2010).
[28] G. Winter, D. G. Waterman, J. M. Parkhurst, A. S. Brewster, R. J. Gildea, M. Gerstel, L. Fuentes-Montero, M. Vollmar, T. Michels-Clark, I. D. Young *et al.*, Acta Crystallogr., Sect. D: Struct. Biol. **74**, 85 (2018).
[29] S. Bruker and B. A. Smart, Acta Crystallogr., Sect. A: Found. Adv. **64**, 112 (2008).
[30] G. M. Sheldrick, Acta Crystallogr., Sect. A: Found. Adv. **71**, 3 (2015).
[31] G. M. Sheldrick, Acta Crystallogr., Sect. C: Struct. Chem. **71**, 3 (2015).
[32] O. V. Dolomanov, L. J. Bourhis, R. J. Gildea, J. A. Howard, and H. Puschmann, J. Appl. Crystallogr. **42**, 339 (2009).
[33] R. D. Shannon, Acta Crystallogr., Sect. A: Found. Adv. **32**, 751 (1976).
[34] A. A. Coelho, Bruker AXS, Karlsruhe, Germany, 2012.
[35] E. Bunting, J. Am. Ceram. Soc. **13**, 5 (1930).
[36] T. Adams, A. Chacon, M. Wagner, A. Bauer, G. Brandl, B. Pedersen, H. Berger, P. Lemmens, and C. Pfleiderer, Phys. Rev. Lett. **108**, 237204 (2012).
[37] S. Blundell, Contemp. Phys. **40**, 175 (1999).
[38] A. Yaouanc and P. D. De Réotier, *Muon Spin Rotation, Relaxation, and Resonance: Applications to Condensed Matter* (Oxford University Press, Oxford, 2011).
[39] R. H. Heffner, J. E. Sonier, D. E. MacLaughlin, G. J. Nieuwenhuys, G. Ehlers, F. Mezei, S.-W. Cheong, J. S. Gardner, and H. Röder, Phys. Rev. Lett. **85**, 3285 (2000).
[40] http://wrap.warwick.ac.uk/110291.